

Patterned Monolayers of Neutral and Charged Functionalized Manganese Arene Complexes on a Highly Ordered Pyrolytic Graphite Surface**

Sang Bok Kim, Robert D. Pike, Jason S. D'Acchioli, Brennan J. Walder, Gene B. Carpenter, and Dwight A. Sweigart*

Controlling the assembly of 2D nanostructures at liquid–solid interfaces is a subject of significant interest for the efficient production of molecular devices, such as sensors and circuits. Self-assembly or self-organization based on specific interactions between molecules allows nanopatterning on a surface and the concomitant fabrication of nanoarchitectures.^[1] 3D crystal engineering aims to predict nanostructures from the mere knowledge of the structure of the components. The most common interactions are hydrogen bonding and metal–ligand coordination to a nitrogen- or carboxylate-oxygen-based ligand. The ligands utilized in 3D work are generally inexpensive and have well-defined directionality and selectivity characteristics. Extensive research on 3D crystal engineering^[2–4] may aid the understanding of 2D structures on surfaces.

Scanning tunneling microscopy has been widely used as a powerful tool for visualizing 2D structures of monolayers and for studying surface features with submolecular resolution. Although supramolecular chemistry involving hydrogen bonding, hydrophobic interactions, and metal–ligand-bond formation has been well studied in solution, this knowledge can not be directly applied to 2D structures on surfaces.^[5–10] The 2D ordering is a compromise between the intermolecular interactions and the minimization of the surface free energy. The fabrication of metal–ligand nanostructures on surfaces has been demonstrated, including copper–pyridyl and iron–carboxylate coordination systems on a Cu(100) substrate.^[11] Metal complexes of pyridine derivatives have been shown to

form ordered nanostructures on a highly ordered pyrolytic graphite (HOPG) surface.^[3] In both of these cases, the 2D nanostructure depends on the directing ability of the metal center and the structure of the carboxylate or pyridine ligands.

Other STM studies of various kinds of metal complexes have been carried out including [bis[(C_n)salicylidene]ethylenediaminato]nickel(II) on HOPG,^[12] potassium-ion-included dibenzo[18]crown-6 on Au,^[13] *trans*-carbonylchlorobis(triphenylphosphino)rhodium(I) on Au,^[14] Ni tetraphenylporphyrin complexes on Au, perfluorinated cobalt phthalocyanine on Au,^[6] oligonucleotide–Rh complexes on HOPG,^[15] dinuclear Ru complexes on Au(111),^[16] organometallic Au and Ir complexes on TiO₂(110) and Si(111),^[17] and Cu–organic polyhedra (MOP) on HOPG.^[18]

To date, the fabrication of metal–ligand complex nanostructures on surfaces have, to our knowledge, all involved complexes that have carboxylates, nitrogen from amines or pyridines, or oxygen from ethers and alcohols as the ligand donor atoms. There have been no reports of 2D nanostructure fabrication involving organometallic arene-bonded complexes. Such systems are especially interesting because the arene ligand is available to interact with the surface. In the case of HOPG, the graphitic surface is likely to bind the organometallic species through a π – π interaction.

Herein, we report the synthesis and crystal structure of [Mn(η^5 -2,5-didodecoxy-1,4-semiquinone)(CO)₃] and demonstrate its binding to a HOPG surface. Quinonoid complexes of manganese tricarbonyl complexes have been studied extensively. For example, [(η^5 -semiquinone)Mn(CO)₃] forms a 1D polymer through hydrogen bonding.^[19] Anionic [(η^4 -quinone)Mn(CO)₃][–] binds to metals through the quinone oxygen atoms to afford 1D, 2D, and 3D coordination polymers (MOFs).^[20] The fabrication of 2D structures on surfaces with metal quinonoid complexes has, heretofore, not been attempted. Although semiquinone manganese tricarbonyl itself has very limited solubility, owing to intermolecular hydrogen bonding, it can be rendered highly soluble in organic solvents by functionalization of the arene with long-chain alkyl substituents. An advantage of arene manganese tricarbonyl complexes lies in the possibility of replacing one of the carbonyl ligands with other functional ligands. Furthermore, the arene itself can be functionalized,^[21] which means that the quinonoid manganese tricarbonyl system can be elaborated into a variety of modified forms. Another generic advantage of quinonoid manganese tricarbonyl complexes is that the charge on the complex can be switched from

[*] S. B. Kim, Prof. G. B. Carpenter, Prof. D. A. Sweigart
Department of Chemistry, Brown University
Providence, RI 02912 (USA)
Fax: (+1) 401-863-9046
E-mail: Dwight_Sweigart@Brown.edu

Prof. R. D. Pike
Department of Chemistry, College of William & Mary
Williamsburg, VA 23187-8795 (USA)

Prof. J. S. D'Acchioli, B. J. Walder
Department of Chemistry, University of Wisconsin–Stevens Point
Stevens Point, WI 54481 (USA)

[**] We are grateful to the donors of the Petroleum Fund, administered by the American Chemical Society, and to the National Science Foundation (CHE-0308640) for support of this research. It is a pleasure to acknowledge Prof. Matthew Zimmt of Brown University and his students, Yanhu Wei, Xiaoliang Wei, and Wenjun Tong for help and discussions concerning the STM results.

Supporting information for this article is available on the WWW under <http://dx.doi.org/10.1002/anie.200805760>.

positive to neutral and even to negative by sequential deprotonation of the η^6 -arene complex, without affecting the metal.^[19] The construction of 2D structures by the use of quinonoid organometallic complexes is expected to prove generally possible, and not limited to manganese complexes. In particular, the use of catalytically active metals, such as Ru and Rh, to construct such systems should be possible. Additionally, the general arene metal tricarbonyl complex system can be neutral or positive, depending on the nature of the metal center.^[22]

Herein, we report the formation of 2D metal–organic systems on a HOPG surface. In particular, $[\text{Mn}(\eta^5\text{-2,5-didodecoxy-1,4-semiquinone})(\text{CO})_3]$ has very strong intermolecular hydrogen bonding and also displays pronounced alkyl chain interdigitation on the HOPG surface. To study a positively charged arene metal complex on the surface, $[(\eta^6\text{-1,4-dioctyloxybenzene})\text{Mn}(\text{CO})_3][\text{BF}_4]$ was synthesized and its 2D structure on HOPG determined, with hydrophobic interactions between the long carbon chains as well as an electrostatic interaction between the positively charged complex and counteranion.

In the 3D crystalline state, $[\text{Mn}(\eta^5\text{-2,5-didodecoxy-1,4-semiquinone})(\text{CO})_3]$ contained two independent molecules, both with a semiquinone manganese tricarbonyl (SQMTC)^[21] core and two dodecoxy substituents at the 2- and 5- positions. In the molecule based on Mn1 (Figure 1 a), one, all-*trans*, hydrocarbon chain is nearly in the plane of the hydroquinone, whereas the other chain is nearly orthogonal to the plane of the ring, as a result of an approximately 90° twist about the bond between the first and second carbon atoms. In the

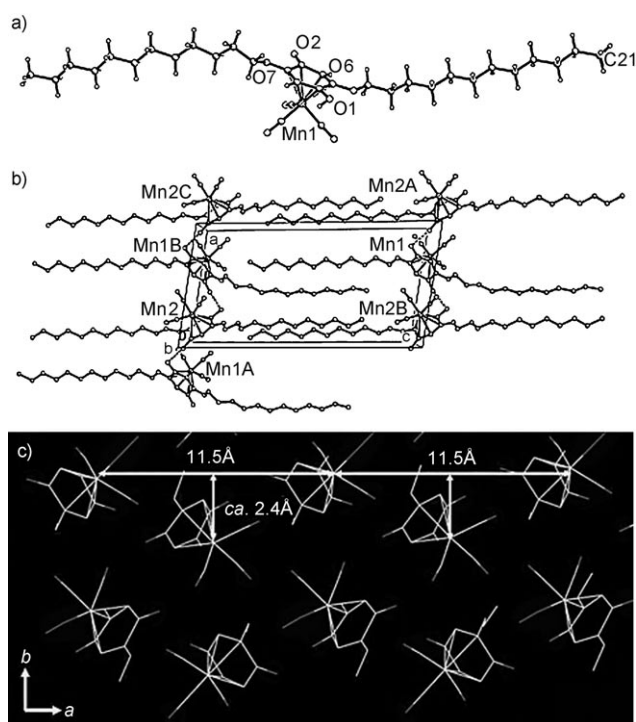


Figure 1. a) X-ray single-crystal structure of $[\text{Mn}(\eta^5\text{-2,5-didodecoxy-1,4-semiquinone})(\text{CO})_3]$; b) the spatial arrangement of the molecules in the *ac* plane in the crystal; c) stacking of 2D layers along the *b* axis direction.

molecule based on Mn2, both side chains are in a plane roughly orthogonal to the ring plane. One chain starts in the plane, but makes a twist of approximately 90° around the bond between the third and fourth carbon atoms; the other side chain is twisted mainly about the bond between the oxygen atom and a ring carbon atom. The two differently oriented molecules are linked into chains by strong hydrogen bonds from hydroxy to the carbonyl oxygen of the semiquinone. The chains of SQMTC cores run along the *a* axis direction and the side chains extend in both directions along the *c* axis, thus forming a ribbon. Side chains from an adjacent ribbon, related to the first by an inversion center between them, interdigitate with those of the first. The consequence is a layer of molecules held together by H bonds and “hydrophobic” interactions (Figure 1 b). These layers stack together more loosely in the *b* direction to form the 3D structure (Figure 1 c).

Figure 2 a and b depict representative STM images of $[\text{Mn}(\eta^5\text{-2,5-didodecoxy-1,4-semiquinone})(\text{CO})_3]$ adsorbed at

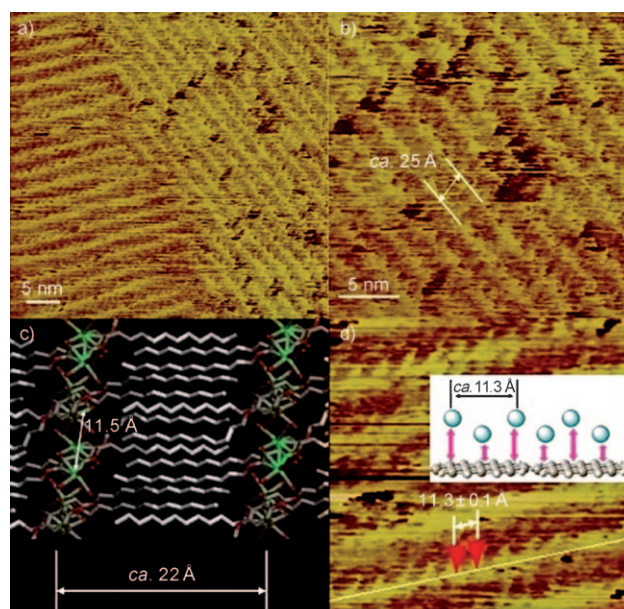


Figure 2. STM image of $[\text{Mn}(\eta^5\text{-2,5-didodecoxy-1,4-semiquinone})(\text{CO})_3]$ on HOPG (25 °C, ambient pressure) at $I_{\text{set}} = 100$ pA and $V_{\text{bias}} = 1$ V. a) large-scale image (50×50 nm²); b) enlarged image (25×25 nm²). The distance between the rows ≈ 25 Å; c) X-ray single-crystal structure of $[\text{Mn}(\eta^5\text{-2,5-didodecoxy-1,4-semiquinone})(\text{CO})_3]$ on *a* and *c* axes. All hydrogen atoms are omitted for clarity. C gray, Mn green, O red; d) enlarged image (15×15 nm²). Center-to-center distance between adjacent bright spots in a row = 11.3 ± 0.1 Å. Inset: schematic diagram of Mn atoms on the surface of HOPG.

the interface between HOPG and a solution of $[\text{Mn}(\eta^5\text{-2,5-didodecoxy-1,4-semiquinone})(\text{CO})_3]$ in phenyloctane. The images clearly show that $[\text{Mn}(\eta^5\text{-2,5-didodecoxy-1,4-semiquinone})(\text{CO})_3]$ forms a 2D structure on HOPG. Whereas the bright contrast indicates a large tunneling current through the $\{(\eta^5\text{-semiquinone})\text{Mn}(\text{CO})_3\}$ moieties of the adsorbed molecules, the hydrocarbon groups are dim. The distance between

the rows was measured to be $25 \pm 1 \text{ \AA}$, which is close to that found in the X-ray crystal structure for the intermolecular distance between arene manganese carbonyl moieties in the *ac* plane, 22.3 \AA (the length of the *c* axis in the unit cell; Figure 2c).

It is reasonable that the distance between the rows (bright) differ somewhat from the intermolecular distance between the $\{(\eta^5\text{-semiquinone})\text{Mn}(\text{CO})_3\}$ moieties along the *c* axis in the crystal. On the HOPG surface, an additional π - π interaction is expected, which is not present in the crystalline state.

The center-to-center distance between bright spots within the same row is $11.3 \pm 0.1 \text{ \AA}$ (Figure 2d). This distance is in agreement with the value of 11.5 \AA for the Mn–Mn distance (Figure 1c) of every other $(\eta^5\text{-semiquinone})\text{Mn}(\text{CO})_3$ moiety on the *a* axis of the crystal. The reason why the center-to-center distance ($11.3 \pm 0.1 \text{ \AA}$) between bright spots in the STM image is almost the same as the Mn–Mn distance of alternate $\{(\eta^5\text{-semiquinone})\text{Mn}(\text{CO})_3\}$ moieties in the crystal may be due to a difference in the height from the HOPG surface of the adjacent $\{(\eta^5\text{-semiquinone})\text{Mn}(\text{CO})_3\}$. In the crystal structure, the Mn of one $\{(\eta^5\text{-semiquinone})\text{Mn}(\text{CO})_3\}$ group is higher than the adjacent $\{(\eta^5\text{-semiquinone})\text{Mn}(\text{CO})_3\}$ group by roughly 2.4 \AA in an “up and down” sequence that repeats along the *a* axis (Figure 1c). It seems likely that the difference in the brightness in a row in the STM image is closely related to the distance from the HOPG surface to the Mn center of the $\{(\eta^5\text{-semiquinone})\text{Mn}(\text{CO})_3\}$ moieties, and that the periodicity ($11.3 \pm 0.1 \text{ \AA}$) in the STM image (Figure 2d) is related to the “higher” $\{(\eta^5\text{-semiquinone})\text{Mn}(\text{CO})_3\}$ moieties rather than the “lower” ones. It is likely that intermolecular hydrogen bonding is more important than the π - π interaction between the organometallic complex and the HOPG surface in the observed 2D surface structure. The agreement between the value ($11.3 \pm 0.1 \text{ \AA}$) from the 2D structure on HOPG for the center-to-center distance of the bright spots and the value (11.5 \AA) for the Mn–Mn distance of alternating $\{(\eta^5\text{-semiquinone})\text{Mn}(\text{CO})_3\}$ units along the *a* axis in the 3D crystal structure indicates indirectly that the hydrogen bonding interaction plays an important role in the 2D organization.

Two of the major interactions within the 2D structure of $[(\eta^5\text{-2,5-didodecoxy-1,4-semiquinone})\text{Mn}(\text{CO})_3]$ on HOPG are intermolecular hydrogen bonding of semiquinone units and van der Waals interactions between the alkyl chains and the HOPG surface.^[23] To reduce or remove these two factors, $[(\eta^6\text{-1,4-dioctyloxybenzene})\text{Mn}(\text{CO})_3][\text{BF}_4]$ was synthesized. This complex can not form hydrogen bonds and would have weaker interactions between the alkyl chains and HOPG than $[(\eta^5\text{-2,5-didodecoxy-1,4-semiquinone})\text{Mn}(\text{CO})_3]$ does because the length of the aliphatic tail is shortened from C_{12} to C_8 . In spite of the ionic charge and relatively short alkyl chains, $[(\eta^6\text{-1,4-dioctyloxybenzene})\text{Mn}(\text{CO})_3][\text{BF}_4]$ was sufficiently soluble in phenyloctane to allow a monolayered 2D structure to form on HOPG (Figure 3). The distance between the rows was measured to be approximately 15 \AA . The lamellar width (roughly 15 \AA) fits well with the expected length of the interdigitating C_8 alkyl chains and the aromatic units in accordance with the model used above. The center-to-

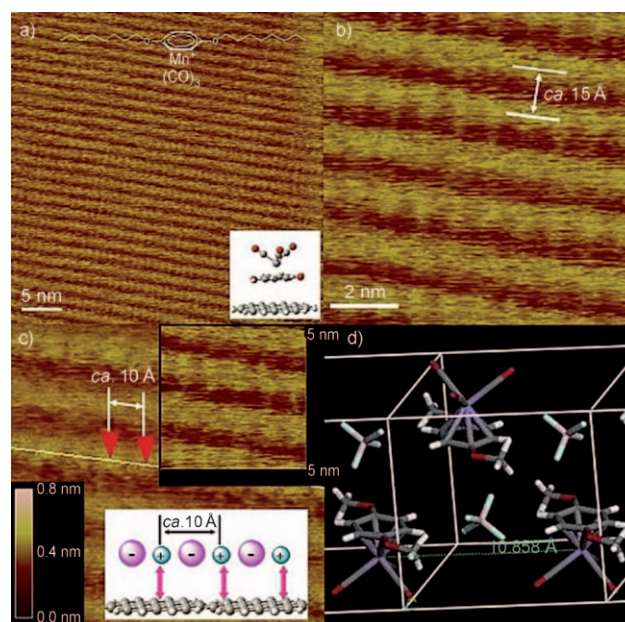


Figure 3. STM image of $[\text{Mn}(\eta^6\text{-1,4-dioctyloxybenzene})(\text{CO})_3][\text{BF}_4]$ on HOPG ($25 \text{ }^\circ\text{C}$, ambient pressure) at $I_{\text{set}} = 80 \text{ pA}$ and $V_{\text{bias}} = 1 \text{ V}$: a) large-scale image ($41 \times 41 \text{ nm}^2$, constant current mode), b) enlarged image ($10 \times 10 \text{ nm}^2$, constant current mode), and c) STM image at constant current mode ($10 \times 10 \text{ nm}^2$) and enlarged image ($5 \times 5 \text{ nm}^2$). The center-to-center distance between adjacent $[\text{Mn}(\eta^6\text{-1,4-dioctyloxybenzene})(\text{CO})_3][\text{BF}_4]$ complexes $\approx 10 \text{ \AA}$. Inset: schematic diagram of Mn ions (small) and BF_4^- counteranions (large) on the surface of HOPG; d) crystal structure of $[(\eta^6\text{-dimethoxybenzene})\text{-Mn}(\text{CO})_3][\text{BF}_4]$. B pink, C gray, F cyan, H white, Mn blue, O red.

center distance between adjacent arene manganese tricarbonyl moieties within the same row is approximately 10 \AA .

Although the BF_4^- counterions could not be seen clearly in the STM image, it can be assumed that BF_4^- anions play a role in connecting each positively charged complex within the same row by electrostatic interactions. To confirm that the BF_4^- counteranions are located between the cationic complexes, the crystal structure of the complex $[(\eta^6\text{-dimethoxybenzene})\text{Mn}(\text{CO})_3][\text{BF}_4]$ was determined. The BF_4^- counteranions are located between the cations and the distance between Mn metals along the *c* axis is 10.9 \AA (Figure 3d). The Mn–Mn distance in the crystal is compatible with the center-to-center distance from the STM image (Figure 3c).

In summary, we have shown that arene manganese tricarbonyl complexes with alkyl chains form monolayered 2D structures on HOPG in two ways; 1) hydrogen bonding and hydrophobic interaction and 2) electrostatic and hydrophobic interaction. In this manner, an ordered array of metal atoms on the surface is attained. Present work is focused on extending studies of 2D structures and modification of the monolayer surface by replacing one of the three coordinated carbonyl ligands with other species. The construction of 2D structures by the use of organometallic arene complexes is expected to prove to be generally possible and not limited to manganese systems. The resultant 2D structure can be tuned by variation of the alkyl chain length and the counterion, if there is one. Correspondingly, this concept should apply to a

variety of catalytically active metals and thereby provide unique opportunities in catalysis.

Experimental Section

Measurements were carried out using a Nanoscope III scanning tunneling microscope (Digital Instruments) operating under ambient conditions at 18 °C. Images were collected at the liquid–solid interface by adding 5–10 μL of solution to the freshly cleaved surface of highly ordered pyrolytic graphite (HOPG, Advanced Ceramics, ZYB Grade) immediately adjacent to the STM tip. Imaging commenced within 5 min. The tip was prepared by cutting a 0.25 mm diameter platinum/rhodium (87/13) wire (Omega). The specific tunneling conditions are given in the Figure captions. The images were analyzed by an external calibration with respect to the basal plane of HOPG (the observed interatomic spacing was compared with the known values). The overall error was then determined to be below $\pm 5\%$. $[\text{Mn}(\eta^6\text{-1,4-dioctaoxybenzene})(\text{CO})_3][\text{BF}_4]$ complex was dissolved in 1-phenyloctane (Aldrich) at below 0.1 mM concentration. The $[\text{Mn}(\eta^5\text{-2,5-didodecoxy-1,4-semiquinone})(\text{CO})_3]$ complex was first dissolved in CH_2Cl_2 followed by dispersion in 1-phenyloctane (below 0.1 mM). The CH_2Cl_2 was allowed to evaporate before STM imaging. STM imaging was performed both at the constant height mode by changing the tunneling parameters (voltage applied to the tip and the average tunneling current) for $[\text{Mn}(\eta^5\text{-2,5-didodecoxy-1,4-semiquinone})(\text{CO})_3]$ and at the constant current mode for $[\text{Mn}(\eta^6\text{-1,4-dioctaoxybenzene})(\text{CO})_3][\text{BF}_4]$. The relative separation at constant current mode and the relative tunneling current at constant height mode between STM tip and the surface are color-coded. At constant current mode, yellow (bright) indicates topographically higher regions of the monolayer (tip withdrawn from the surface) and black (dark) corresponds to topographically lower regions. At constant height mode, yellow indicates higher current generating regions of the monolayer and black corresponds to lower current generating region. CCDC 707879 and 707880 contain the supplementary crystallographic data for this paper. These data can be obtained free of charge from The Cambridge Crystallographic Data Centre via www.ccdc.cam.ac.uk/data_request/cif.

Received: November 26, 2008

Published online: January 28, 2009

Keywords: arene ligands · manganese · monolayers · scanning probe microscopy · surface chemistry

- [1] J. V. Barth, G. Costantini, K. Kern, *Nature* **2005**, *437*, 671.
- [2] A. Mourran, U. Ziener, M. Möller, M. Suarez, J.-M. Lehn, *Langmuir* **2006**, *22*, 7579.
- [3] Y. Kikkawa, E. Koyama, S. Tsuzuki, K. Fujiwara, K. Miyake, H. Tokuhisa, M. Kanesato, *Langmuir* **2006**, *22*, 6910–6914.
- [4] H. Dang, T. Maris, J.-H. Yi, F. Rosei, A. Nanci, J. D. Wuest, *Langmuir* **2007**, *23*, 11980–11985.
- [5] L. C. Giancarlo, G. W. Flynn, *Acc. Chem. Res.* **2000**, *33*, 491–501.
- [6] S. De Feyter, F. C. De Schryver, *Chem. Soc. Rev.* **2003**, *32*, 139–150.
- [7] X. Yang, J. Wang, X. Zhang, Z. Wang, Y. Wang, *Langmuir* **2007**, *23*, 1287–1291.
- [8] S. Xu, M. Dong, E. Rauls, R. Otero, T. R. Linderof, F. Besenbacher, *Nano Lett.* **2006**, *6*, 1434–1438.
- [9] S. De Feyter, A. Gesquière, P. C. M. Grim, F. C. De Schryver, *Langmuir* **1999**, *15*, 2817–2822.
- [10] J. Otsuki, S. Shimizu, M. Fumino, *Langmuir* **2006**, *22*, 6056–6059.
- [11] a) A. Dmitriev, H. Spillman, N. Lin, J. V. Berth, K. Kern, *Angew. Chem.* **2003**, *115*, 2774–2777; *Angew. Chem. Int. Ed.* **2003**, *42*, 2670–2673; b) T. Classen, G. Fratesi, G. Costantini, S. Fabris, F. L. Stadler, C. Kim, S. de Gironcoli, S. Baroni, K. Kern, *Angew. Chem.* **2005**, *117*, 6298–6301; *Angew. Chem. Int. Ed.* **2005**, *44*, 6142–6145; c) A. Langner, S. L. Tait, N. Lin, R. Chandrasekar, M. Ruben, K. Kern, *Angew. Chem.* **2008**, *120*, 8967–8970; *Angew. Chem. Int. Ed.* **2008**, *47*, 8835–8838.
- [12] I. Sakata, K. Miyamura, *Chem. Commun.* **2003**, 156–157.
- [13] A. Ohira, M. Sakata, C. Hirayama, M. Kunitake, *Org. Biomol. Chem.* **2003**, *1*, 251–253.
- [14] X.-S. Zhou, Z.-R. Dong, H.-M. Zhang, J.-W. Yan, J.-X. Gao, B.-W. Mao, *Langmuir* **2007**, *23*, 6819–6826.
- [15] Y. Kim, E. C. Long, J. K. Barton, C. M. Lieber, *Langmuir* **1992**, *8*, 496–500.
- [16] Z. Wei, S. Guo, S. A. Kandel, *J. Phys. Chem. B* **2006**, *110*, 21846–21849.
- [17] Y. Maeda, M. Okumura, M. Daté, S. Tsubota, M. Haruta, *Surf. Sci.* **2002**, *514*, 267–272.
- [18] H. Fukawa, J. Kim, K. E. Plass, O. M. Yaghi, *J. Am. Chem. Soc.* **2006**, *128*, 8398–8399.
- [19] M. Oh, G. B. Carpenter, D. A. Sweigart, *Organometallics* **2002**, *21*, 1290–1295.
- [20] a) M. Oh, G. B. Carpenter, D. A. Sweigart, *Angew. Chem.* **2001**, *113*, 3291–3294; *Angew. Chem. Int. Ed.* **2001**, *40*, 3191–3194; b) M. Oh, G. B. Carpenter, D. A. Sweigart, *Angew. Chem.* **2002**, *114*, 3802–3805; *Angew. Chem. Int. Ed.* **2002**, *41*, 3650–3653; c) M. Oh, G. B. Carpenter, D. A. Sweigart, *Angew. Chem.* **2003**, *115*, 2072–2074; *Angew. Chem. Int. Ed.* **2003**, *42*, 2026–2028; d) M. Oh, G. B. Carpenter, D. A. Sweigart, *Acc. Chem. Res.* **2004**, *37*, 1–11; e) J. A. Reingold, S. U. Son, S. B. Kim, C. A. Dullaghan, M. Oh, P. C. Frake, G. B. Carpenter, D. A. Sweigart, *Dalton Trans.* **2006**, 2385–2398.
- [21] a) S.-G. Lee, J.-A. Kim, Y. K. Chung, T.-S. Yoon, N.-J. Kim, W. Shin, *Organometallics* **1995**, *14*, 1023–1029; b) Y. Huang, G. B. Carpenter, Y. K. Chung, B. Y. Lee, D. A. Sweigart, *Organometallics* **1995**, *14*, 1423–1428; c) Y. Cao, K. Woo, L. K. Yeung, G. B. Carpenter, D. A. Sweigart, *Organometallics* **1997**, *16*, 178–183.
- [22] a) S. G. Davies, T. Loveridge, M. F. C. C. Teixeira, J. M. Clough, *J. Chem. Soc. Perkin Trans. 1* **1999**, 3405–3412; b) M. Rosillo, G. Domínguez, L. Casarrubios, J. Pérez-Castells, *J. Org. Chem.* **2005**, *70*, 10611–10614; c) T. T. To, E. J. Heilweil, *J. Phys. Chem. A* **2007**, *111*, 6933–6937; d) H. Kunkely, A. Vogler, *Chem. Commun.* **1998**, 395–396; e) S. Antonini, F. Calderazzo, U. Englert, E. Grigiotti, G. Pamaloni, P. Zanello, *J. Organomet. Chem.* **2004**, *689*, 2158–2168; f) M. V. Baker, M. R. North, *J. Organomet. Chem.* **1998**, *565*, 225–230; g) H. Seo, S.-G. Lee, D. M. Shin, B. K. Hong, S. Hwang, D. S. Chung, Y. K. Chung, *Organometallics* **2002**, *21*, 3417–3425; h) M. Oh, J. A. Reingold, G. B. Carpenter, D. A. Sweigart, *Coord. Chem. Rev.* **2004**, *248*, 561–569; i) C. C. Neto, C. D. Baer, Y. K. Chung, D. A. Sweigart, *J. Chem. Soc. Chem. Commun.* **1993**, 816–818.
- [23] Y. Wei, K. Kannappan, G. W. Flynn, M. B. Zimmt, *J. Am. Chem. Soc.* **2004**, *126*, 5318–5322.
- [24] S. C. Yu, S. Hou, W. K. Chan, *Macromolecules* **2000**, *33*, 3259–3273.